

Prediction of Freezing of Gait from Parkinson's Disease Movement Time Series using Conditional Random Fields

Roland Assam
RWTH Aachen University
Germany
assam@cs.rwth-aachen.de

Thomas Seidl
RWTH Aachen University
Germany
seidl@cs.rwth-aachen.de

ABSTRACT

Freezing of Gait (FOG) in Parkinson's Disease (PD) is a brief episodic impedance of movement that is mostly manifested at the late stages of the PD. Accelerometer sensors are widely utilized to collect dysfunctional movement time series data stemming from patients with PD. In this work, we propose a robust FOG predictive model that employs a combination of wavelets and Conditional Random Fields (CRF) to predict FOG episodes from low level FOG accelerometer time series interleaved with normal movement time series of PD patients. Specifically, in order to derive and extract unique signature features of FOG time series, we utilize wavelets to perform in-depth analysis of PD movement spectral at multiple resolutions. We design a CRF that leverages the extracted signature feature vectors to diligently learn the underlying characteristics of FOG time series and to effectively predict FOG episodes at their onsets. Our empirical evaluations on a real PD dataset demonstrate that our technique delivers enhanced prediction accuracies.

Categories and Subject Descriptors

H.2.8 [Database Management]: Database Applications—*Data mining*

General Terms

Algorithms, theory, experimentation.

Keywords

Freezing of Gait, Time Series Prediction, Wavelets, Conditional Random Fields

1. INTRODUCTION

Parkinson Disease (PD) is a neurological disorder that was discovered in 1817 by James Parkinson. It is caused by the deficiency of striatal dopamine because of the loss of nigrostriatal neurons [5]. The degeneration of the latter neurons disrupts the limbic, visceromotor and sematormotor

Permission to make digital or hard copies of all or part of this work for personal or classroom use is granted without fee provided that copies are not made or distributed for profit or commercial advantage and that copies bear this notice and the full citation on the first page. Copyrights for components of this work owned by others than ACM must be honored. Abstracting with credit is permitted. To copy otherwise, to republish, to post on servers or to redistribute to lists, requires prior specific permission and/or a fee. Request permissions from Permissions@acm.org.

HealthGIS'14, November 04-07 2014, Dallas/Fort Worth, TX, USA

Copyright 2014 ACM 978-1-4503-3136-4/14/11 ...\$15.00.

<http://dx.doi.org/10.1145/2676629.2676630>

systems of the brain [4], causing the limbic and other brain centers to relinquish influence and control of motor neurons. This translates into the dysfunction of the body's motor systems, which is manifested by involuntary trembling of the head, arms and legs. It also causes Bradykinesa (slowness) and "freezing" as the disease evolves.

The aforementioned freezing is mostly experienced at the late stages of the Parkinson's disease [3], and it is coined Freezing of Gait (FOG). FOG is a brief episodic impedance of movement, which is characterized by the inability of a person (at rest) to commence movement. For a moving person, FOG is governed by the abrupt halt in her motion, despite efforts to resume movement. Another hallmark of FOG is the involuntary trembling of the knees. [3] mentioned that FOG episodes are mostly observed when a patient starts moving or during turning movement. They also alluded that FOG episodes occur briefly for up to 10 seconds in most cases but may extend above 30 seconds in a few occasions.

Despite these short durations, FOG takes a PD patient by surprise, thus it requires patient monitoring. Besides, FOG episodes can be accompanied by falls, which might lead to body injuries. Patient monitoring or injuries stemming from falls after FOG episodes might prompt an elevation of the health care cost. The freezes and falls also cause patients to become dependent on others and even discourages them to move, thus depreciating their quality of life. Dopamine-related medications have also not been successful in overcoming FOG [11, 3]. Physicians and patients rely on certain behavioral tactics to dampen the effects of FOG (e.g., walking to music or altering the body weight) [2]. One approach that has been successful in reducing FOG symptoms is the Rhythmic Auditory Simulation (RAS). However, for RAS to work effectively, FOG episodes need to be properly detected or predicted. Since PD is associated with trembling, the movement patterns of such trembles, as well as FOG can be captured by wearable sensors. [2] introduce a wearable device that entails 3D-accelerometer sensors that record the movement time-series of a PD patient.

With the significant drop in the prices and weights of sensors, one approach that has garnered broad scale support to collect and analyze Parkinson disease movement data is the use of accelerometer sensors. It involves the use of sensors for the convenient gathering of movement data from PD patients as they go about their daily life activities. This accelerometer sensor data entails elusive FOG movement patterns that can be uncovered using proper data mining techniques. This can be eventually utilized to identify, detect or

predict FOG in PD. For instance, [2] propose an algorithm that can detect FOG in real-time and provide context-aware RAS to enhance gait in PD.

While other works [11, 6, 2] have proposed techniques to detect FOG in PD from sensors, in this paper, we propose a novel FOG prediction technique that utilizes a combination of wavelets, vector quantization and Conditional Random Fields (CRF) to predict high level FOG events from low level accelerometer time series. A FOG predictor can be used in a broad spectrum of health applications for patient monitoring, to enhance the quality of life for PD patients, and to erode health care cost.

1.1 Our Contributions

Distinguishing low level FOG time series (at its onset) in the midst of normal movement time series is an insidious and challenging problem. It requires the rigorous analysis of PD movement time series obtained from accelerometer sensors. We make two main contributions in this paper. First, we devise a new feature selection approach for PD time series data, which extracts unique signature feature vectors from a FOG time series. The extracted features are employed to effectively discriminate FOG time series from the normal movement time series of PD patients. Specifically, we decompose the time domain PD movement time series using dyadic wavelet transform to obtain its spectral. We then perform in-depth analysis of the PD movement spectral at multiple resolutions to detect elusive patterns within FOG signals. Among others, we observe that at the onset of a FOG signal, there is a significant difference in the wavelet spectral sub-energy between a FOG episode and a normal movement. This spectral energy difference is consistent and sharper at several frequency resolutions. We utilize such findings to derive signature feature vectors, which are employed to identify and distinguish FOG signals from normal signals.

To effectively leverage the selected feature vectors in our predictive model, we first study the probability density of these features, and then cluster densely populated feature vectors into several regions called voronoi regions through the process of vector quantization. We represent nearest neighboring feature vector values in a given voronoi region with the centroids of the given regions. All the resulting centroids are utilized to create a codebook. We perform vector quantization using the Linde-Buzo-Gray (LBG) algorithm [8].

Our second contribution involves the proposal of a robust FOG predictive model, which utilizes the aforementioned wavelet feature vectors, the codebook, and the CRF, to predict an FOG episode at its onset with a high veracity. In particular, we utilize the wavelet spectral features and the codebook to train our CRF to find hidden trends from the time series. Our CRF learns the underlying characteristic of an FOG time series during gradient ascent and assigns weights to re-occurring patterns. In the testing phase, our CRF utilizes the learned knowledge to determine FOG in Parkinson’s disease with an enhance accuracy. Using a Parkinson’s disease accelerometer sensor dataset [2], our empirical evaluation illustrates that our technique delivers a high prediction performance of more than 90% depending on the sample window size.

The remainder of this paper is organized as follows. Sub-section 1.2 discusses relevant related works while Section 2.1

describes the PD data acquisition process, the accelerometer sensor dataset and formally defines the problem of FOG prediction. In Section 3, we introduce a feature extraction approach for PD time series using dyadic wavelet transform, whereas in Section 4, we present our CRF predictive model. Section 5 provides the empirical results of our conducted experiments. We conclude in Section 6.

1.2 Related work

[6] propose a technique that employs wavelet to extract feature vectors from EEG signals. They then use Back Propagation Neural Network classifier and the extracted features to classify FOG from the EEG signals. Our approach differs from this work because we utilize CRF. Also, the study performed by [6] is based on EEG signal while our work explores accelerometer signals. [2] propose a technique that detects FOG episodes from accelerometer data in real time. If their technique identifies a FOG episode, it sends a message to an RAS which triggers the patient to continue moving.

[11] presented a FOG detection technique that is based on a freeze threshold term the Freeze Index. They derive the latter index by examining the power spectra of vertical linear acceleration. Our technique differs from this approach in that we utilize wavelet and CRF to identify and predict FOG episode. [6, 2, 1, 11] focuses on the detection of FOG in Parkinson’s disease. However, FOG also occurs in other neuro-related diseases.

2. PRELIMINARIES

2.1 Data Acquisition and Problem Definition

We utilize the Daphnet Freezing of Gait dataset which was collected and made public by [2]. The data gathering process was geared to capture FOG from wearable accelerometer sensors. Prior to describing the accelerometer sensor data, we first highlight the data collection process. The data was collected at the Laboratory for Gait and Neurodynamics at Tel Aviv Sourasky Medical Center. The data was gathered from 10 PD patients, 7 males and 3 females ranging from the age of 59 to 75 years with different stages of PD. Two patients had frequent FOG episodes. During data acquisition, apart from the aforementioned two patients, all patients were on the off stage of their medication cycle.

The 10 patients were requested to carry out three movement patterns. These include, 1) walking in a straight line, 2) walking randomly including the simulation of 360 degrees turns, 3) daily life walking pattern which involves the deliberate movement from rooms to rooms, such as picking up a coffee and back. In addition, while the patients were moving, their movements were simultaneously video taped by a physiotherapist to capture all FOG episodes. Another physiotherapist labeled the current activity of each patient as standing, walking, turning or freezing. After all data was collected, the physiotherapists analyzed the video and combined it with the manually labeled movements to create the ground truth labels. They also used them to determine the start times, end times and durations of the FOG episodes.

Three 3D-accelerometer sensors were used to record the movements of each patient at a sampling rate of 64 Hz. One sensor was attached around the ankle, the other above the knee, and the third accelerometer sensor was placed on a belt and wrapped around the hip of a patient. An accelerometer measures the acceleration and orientation of the PD pa-

tients’ movements on three axes or dimensions. Namely, the X, Y and Z axis. The X-axis collects readings about the horizontal forward motion of a subject, whereas the upward and downward movements are captured by the Y-axis. In contrast, the Z-axis records the movement in the horizontal lateral direction.

While four movement activities (i.e., standing, walking, turning and freezing) were manually labeled by the physiotherapists, the labels of standing, walking and turning were categorized as "no freezing". As a result, the final ground truth class labels for each 3D-accelerometer sensor reading (of the publicly available Daphnet dataset) is either "freezing" or "no freezing". Throughout this work, we refer to the "freezing" class as the *FOG label*, whereas the "no freezing" class is called the *normal label*. [2] reported that 8 out of the 10 patients experienced FOG during the data gathering process.

2.2 Problem Definition

Prior to the presentation of our FOG prediction technique, we begin by formally articulating the problem we aspire to solve in this paper. Consider that we are provided with 3D-accelerometer sensor readings stemming from the sensors described in Section 2.1, which encapsulates the movement time series of PD patients. The prime rational of this paper is to craft a predictive model that predicts a high level FOG episode from a low level sensor time series data at the onset of the FOG episode. We should note that it is important to predict FOG immediately as it starts, so that the predicted results can be used by other systems (e.g., RAS) to alert the patient or perform certain actions that can suppress the FOG episode.

DEFINITION 1. (PROBLEM DEFINITION): *Consider a finite set $\mathcal{E} = \{e_1, e_2\}$ of movement classes, where e_1 denotes the normal movement and e_2 represents the FOG episode. Given \mathcal{E} and an ordered observation sequence of accelerometer sensor movement time series $\mathcal{O} = \{o_1, o_2, \dots, o_n\}$, where each $o_i \in \mathcal{O}$ represents three tri-axial accelerometer points from three different sensors, and each tri-axial point $p_s(x_i, y_i, z_i)$ denotes a point from sensor s at time t_i , and $t_1 < t_2 < t_i$, predict the Parkinson’s disease movement label $e_j \in \mathcal{E}$ that corresponds to the observation sequence \mathcal{O} within a threshold time τ .*

To solve the problem in Definition 1, we propose a robust FOG predictor that employs a novel combination of dyadic wavelet transform, vector quantization and CRF to identify and predict FOG episodes time series that are sandwiched within normal movement time series of PD patients. At a higher level, given the multi-sensor accelerometer data described in Section 2.1, we first extract valuable feature vectors that can be used to distinguish FOG time series from normal movement time series by performing multi-resolution wavelet decomposition through wavelet transform. Unlike the Fourier transform which can analyze signals only in either the time domain or frequency domain, wavelet transform enables us to analyze the movement of PD patients in both the time and frequency domain at the same time. During the spectral analysis of the collected time series, we extract signature features that can effectively discriminate FOG episodes from normal signals. After the collection of all important feature vectors, we generate a codebook using vector quantization to obtain centroids of neighboring feature vec-

tors. Subsequently, the extracted feature vectors are represented by their centroids. Finally, we then utilize CRF, known for its strong inference probability to predict a FOG given a sequence of codebook centroids.

In what follows, we present a technique to select vital features vectors using wavelets in Section 3.2, and utilize the extracted features for the design of a codebook using vector quantization in Section 3.4.

3. DATA ANALYSIS

3.1 Fundamentals of Wavelet Transform

There are two major kinds of wavelet transforms. Namely, Continuous Wavelet Transform (CWT) and Discrete Wavelet Transform (DWT). A mother wavelet is required to perform wavelet transform. Wavelet transform is achieved by the dilation and translation of a mother wavelet $\psi(x)$. In this work, we utilize dyadic wavelets to extract feature vectors for FOG prediction. Dyadic wavelets are also known as Maximum Overlap Discrete Wavelet Transform (MODWT) or Undecimated Wavelet Transform. Dyadic wavelet is a slight mutation of DWT, hence they can be better described by first introducing DWT.

The DWT of a function $f(x)$ is given by

$$DWT_{\psi} f(j, \tau) = \int_{-\infty}^{+\infty} f(x) \psi_{j, \tau}^*(x) dx \quad (1)$$

where $\psi_{j, \tau} = \frac{1}{2^j} \cdot \psi\left(\frac{x-\tau}{2^j}\right)$, $j \in \mathbb{Z}$ is the dilation or scale, $\tau \in \mathbb{Z}$ is the translation and $\psi^*(..)$ is the complex conjugate of the mother wavelet. The mother wavelet is given by $\psi(x)$ and when scaled with j , it yields a scaling function ψ_j .

DWT decomposes a signal into fine and coarse wavelet coefficients at different resolutions or scales. Multi-Resolution Analysis (MRA) using DWT can be accomplished by employing the algorithm proposed by Mallat [10]. The decomposition of a sequence or signal starts at a scale $J = \log_2(N) - 1$, where N is the length of the sequence. At each scale j , DWT yields a fine coefficient called the approximation coefficient a_j and a coarse coefficient termed the detail coefficient d_j . We will utilize some of these coefficients as feature vectors for FOG prediction. The approximation coefficients correspond to the low pass filter h while the detail coefficients correspond to the high pass filter g . The algorithm iteratively moves from a higher scale j to a scale $j - 1$. At each lower scale $j - 1$, the signal is subdivided into low pass signal and high pass signal, and they are then down-sampled. Down-sampling involves the reduction of the number of samples of the signal by half of its original size. The iteration continues and terminates at $j = 0$.

A major difference between MODWT and DWT is that there is no down-sampling for MODWT. As a result, MODWT consists of redundant features. In addition, while DWT requires that the size of the input data be a multiple of a power of two, MODWT has no restriction on the signal length, thus making it more practical to utilize.

3.2 Feature Extraction

In this work, to extract features, for each of the three sensors, we first determine a resultant 1D signal from the 3D accelerometer sensor reading (i.e., the signals of the x, y, z -axis) and analyze it separately. The formula for the resultant signal is provided and discussed in Section 4.3. We depict each 1D resultant signal as a collection of data points in the

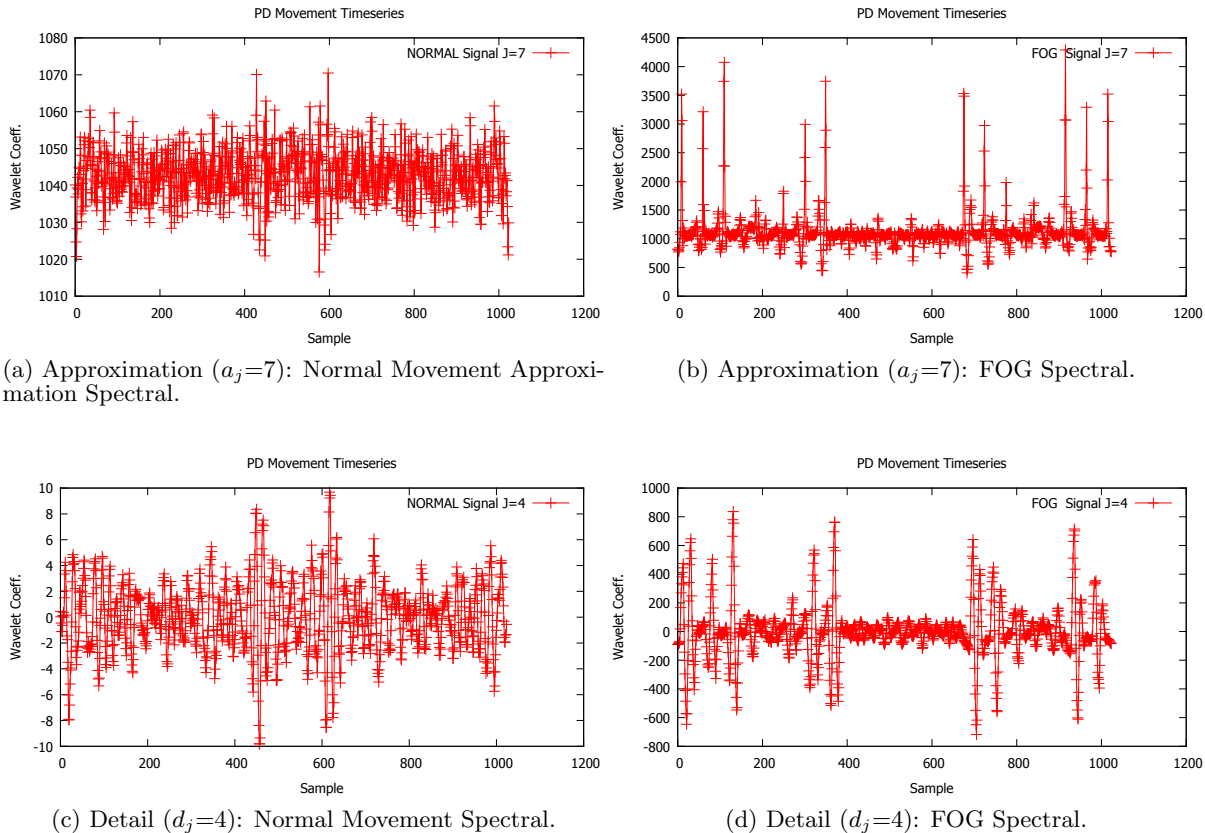


Figure 1: Ankle Sensor: Parkinson's Disease Movement Spectral Analysis.

time domain. In digital signal processing, it is known that the most important characteristics of a signal lie in the frequency domain. Towards this end, we perform multi-scale wavelet transform decomposition of each of the 1D resultant time domain accelerometer reading. Specifically, we commence the decomposition of the 1D accelerometer signal using the Daubechies 4 mother wavelet. At each scale j , the MODWT generates an the approximation coefficient a_j which corresponds to the low pass filter h and a detail coefficient d_j that corresponds to the high pass filter g . For instance, Figure 1 and Figure 3 illustrate the spectral of a decomposed resultant FOG time series and a normal movement time series of a PD patient for the ankle and hips sensors, respectively. For each sensor type, we perform pairwise analysis of each FOG time series with its corresponding normal movement time series at a given scale j to determine important feature vectors. To accomplish this, we record all the approximation and detail wavelet coefficients instituted at each scale until the iteration stops at scale $j = 0$. After the complete decomposition of the 1D signal which is associated with the production of wavelet coefficients, we extract and utilize a unique combination of the produced wavelet coefficients as feature vectors of our FOG prediction technique.

We repeat the same MODWT decomposition of the resultant time-domain accelerometer signals for the other sensors, and extract signature feature vectors that can be utilized to effectively differentiate an FOG episode from a normal movement time series, as articulated in the next section.

3.3 Feature Vector Selection

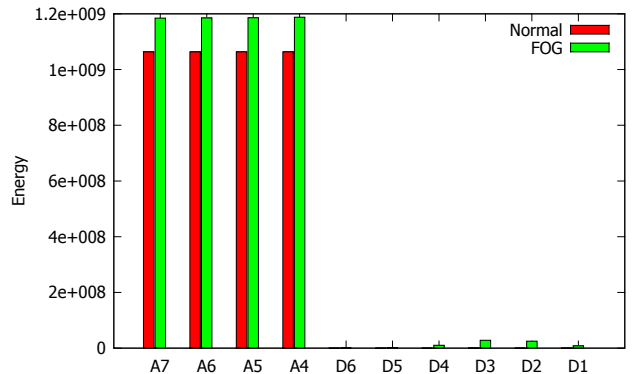
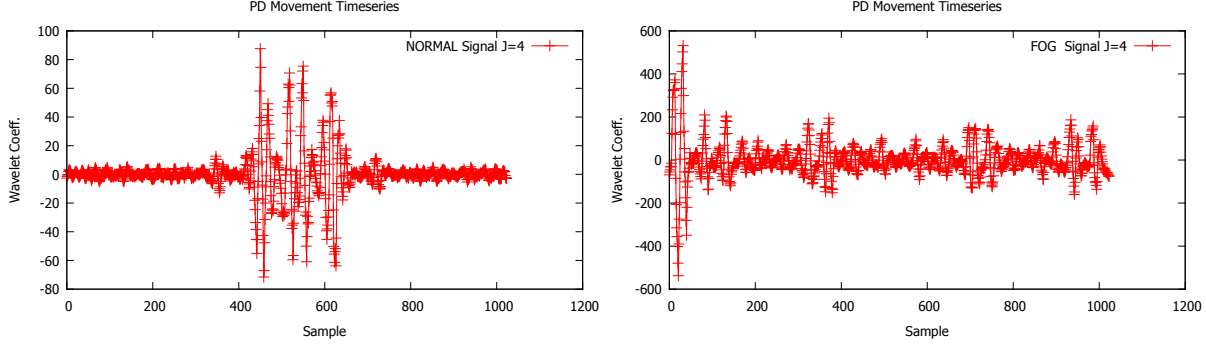


Figure 2: Ankle Sensor: Wavelet approximation and detail sub-band energies for FOG and Normal Movement.

Approximation Coefficients: During our rigorous analysis of PD movement time series to find unique features that can distinguish an FOG episode time series from a "no freeze" (i.e., normal) time series, we observe that the FOG sub-band energies of the approximation and detail wavelet coefficients were significantly higher than that of the normal movement time series as shown in Figure 2 and Figure 4. For the approximation coefficients, we investigated the decay of the sub-band energies across scales to avoid selecting sub-band energies that are corrupted by noise. While the approximation sub-band energies at scale $j = 7$, $j = 6$ and $j = 5$ could be used as good feature vectors, (since their sub-band energies



(a) Detail ($d_j=4$): Normal Movement Spectral .

(b) Detail($d_j=4$): FOG Detail Spectral.

Figure 3: Hip Sensor: Parkinson's Disease Movement Detail Spectral Analysis.

can be employed to differentiate FOG from normal time series,) we choose the approximation sub-band energy at scale $j = 4$ as our approximation feature vector for two reasons. First, they are less susceptible to be corrupted by random noise. Secondly, we aspire to detect FOG at its onset, this means, we anticipate to encounter scenarios where the sample sizes of the time domain signals to be decomposed can be as small as 170 points, hence the maximum j will be less than 7.

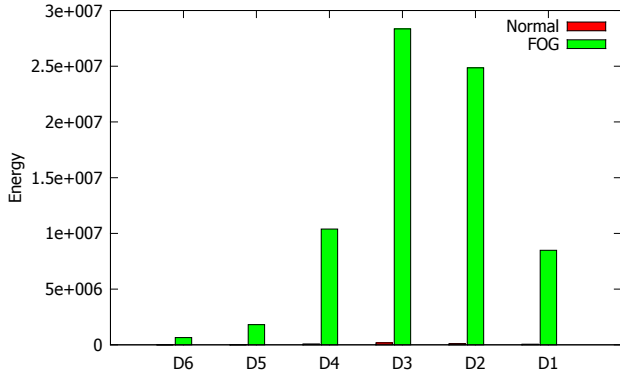


Figure 4: Ankle Sensor: Wavelet detail sub-band energies for FOG and Normal Movement.

For all sensors, we compute the approximation sub-band energies for $j = 4$. These approximation sub-band energies are extracted and utilized as feature vectors.

Detail Coefficients: During our analysis of the detail wavelet coefficients, we observe that they comprise of salient regions that hold unique characteristics of the signal and can be utilized to effectively discriminate normal movements from FOG episodes. For instance, Figure 4 shows the energy distribution from the detail wavelet coefficients.

As can be seen in Figure 4, the sub-band energies from scale $j = 4$ to $j = 1$ of an FOG time series is profoundly higher than that of a normal time series. In fact, their relative differences are higher than those manifested by the approximations wavelet coefficients. As a result, to capture and segregate FOG point sequences from normal movements, we select the detail wavelet coefficients from scale $j = 4$ to $j = 1$ (i.e., $d_j = \{d_4, d_3, d_2, d_1\}$), compute their detail sub-band energies, and utilize them as feature vectors.

In summary, for each 1D decomposed accelerometer sig-

nal, we select its approximation wavelet coefficients at scale $j = 4$ and its detail wavelet coefficients at scales $j = 4$ to $j = 1$. The approximation and detail sub-band energies are then computed from the selected coefficients and utilized as feature vectors for our FOG prediction technique. Hence, five features are extracted from each sensor. Since there are three accelerometer sensors, the total amount of feature vectors used is 15. In the next sections, we will describe how these feature vectors are employed for FOG prediction.

3.4 Vector Quantization of Wavelet Feature Vectors

The wavelet feature vectors collected in the previous section consist of continuous feature vector values of the signals. Most of these values are unique. We utilize vector quantization to eliminate redundancy and study the linear and non-linear relationships between these feature vectors, as well as their probability density functions. Specifically, we employ vector quantization to approximate these continuous feature vector values before they are used by the CRF for prediction.

Given that $x = \{x_1, x_2, \dots, x_d\}$ is our d -dimensional real-valued wavelet feature vector where $d = 15$, vector quantization is the processes of mapping the wavelet feature vectors x to another d -dimensional real-valued vector y . At such, we say x is quantized by y . y is called a codeword and a finite set of codewords is called a codebook $C = \{y_i : i = 1, 2, 3, \dots, L\}$. The size of the codebook is denoted by L and it corresponds to the number of codewords in a codebook C . Each codeword y_i corresponds to the centroid of a region or cell called the voronoi region.

To build a codebook for our wavelet feature vectors, we explore a codebook size of $L = 32$ and $L = 64$, and employ the Linde-Buzo-Gray (LBG)[8] vector quantization algorithm to partition the vector space \mathcal{R}^d into L regions or cells. This leads to the creation of several voronoi regions and their corresponding codewords, which represent the centroids of the voronoi regions. For each region C_i , we quantize any wavelet feature vectors in that region as codeword of y_i of C_i . That is, we represent all feature vectors within a region with the codeword of the region. In the next section, during the prediction of the onset of an FOG episode, all wavelet feature vectors will be represented by their nearest neighboring codewords.

4. FOG PREDICTIVE MODEL

4.1 CRF Introduction and FOG Modeling

A CRF [7] is a discriminative probabilistic graphical model that can be utilized for statistical inference. It performs inference by mapping an observation sequence X to a sequence of labels Y . For the FOG prediction problem, we model our CRF as follows. Given a dataset D consisting of all low level Parkinson’s disease accelerometer sensor readings, after extracting signature spectral features through dyadic wavelet transform and the vector quantization of the extracted spectral feature vectors has been performed, we replace each wavelet feature value with its corresponding centroid. Then, we align the feature vectors from each reading of all the three accelerometer sensors as an ordered observation sequence of centroids $X = \{x_1, x_2 \dots x_T\}$, where each x_i denotes a centroid. Also, we create a set of candidate labels $Y = \{y_1, y_2\}$, where y_1 refers to ”no freezing” (i.e., normal movement) and y_2 denotes freezing (i.e., an FOG episode). Generally, CRFs are employed to determine the conditional probability of Y given an observation sequence X (i.e., $P(Y|X)$).

To determine $P(Y|X)$ in a CRF, an undirected graph is described using fully connected sub-graphs. Specifically, a CRF is an undirected graph $G = (V, E)$ with edges from y_{i-1} to y_i , as well as edges from a state y_i to any observation in X . The edges of a CRF forms a fully connected sub-graphs called a clique. The maximal clique C of a graph G can be employed to compute the probability distribution of an undirected graph. Specifically, the probability of an undirected graph can be derived from the product of potential functions $\Psi(c)$ for each clique c over G . This is given by

$$P(V) = \frac{1}{Z} \prod_c \Psi(c) \quad (2)$$

where Z is the normalization factor which ensures that the probabilities sum to one. In this work, we utilize a linear chain CRF for FOG recognition. Since the cliques of a CRF comprises of edges with y_{i-1} , y_i and X , the potential function for each clique in a linear chain CRF is given by $\Psi(c) = \exp(i, y_{i-1}, y_i, X)$. Hence, $P(Y|X)$ is given by

$$P(Y|X) = \frac{1}{Z(X)} \exp\left(w_a \cdot \prod_{i=1}^I f_a(i, y_{i-1}, y_i, X)\right) \quad (3)$$

where w is the feature weight and $Z(X)$ is the normalization factor which ensures that the probabilities sum to one. f is the feature function. In the next section, we describe how f is used for FOG prediction.

4.2 FOG Characteristics as CRF Features

Given a training dataset consisting of multiple sequence of spectral centroids that originate from 3 accelerometer sensors, our CRF learns the characteristics of the underlying data by searching hidden patterns. That is, it searches for elusive patterns from each sequence of centroids by investigating the Markov property between two random centroid variables. If a sequence occurs frequently and always result to the same output y_i , the behavior is stored using the feature function f and the behavior is investigated in other centroid sequences. At the end of the data exploration process by our CRF, numerous characteristics detected by different feature functions are found. We should note that if a feature occurs, we embed the feature to our CRF by assigning a real value number of 1. Otherwise, zero is added.

4.3 Modeling FOG Sequences

To model our predictor, we formulate the problem of FOG prediction as a sequential labeling task. Given an observation sequence O of centroids that represent vital signature feature vectors of an FOG or normal time series, the objective is to find the most probable movement class, which could have generated the observation sequence O .

Observation: As a recap, an accelerometer sensor measures the 3D motions of the subjects (i.e., at the x , y and z axis). The observation of our CRF is derived from the resultant time-domain motion signal \widehat{M}_i of a tri-axial accelerometer reading at a given time i . Formally, \widehat{M}_i is given by Equation 4.

$$\widehat{M}_i = \sqrt{(x_i)^2 + (y_i)^2 + (z_i)^2} \quad (4)$$

Specifically, the observation sequence is derived from \widehat{M}_i by first performing dyadic wavelet transform of \widehat{M}_i and extracting its feature vector. Then, to generate an observation sequence for our CRF, we use the codebook to replace the latter continuous value feature vectors with their nearest centroids. The sequence of the corresponding centroids from the three sensors are used as the observation sequence of our CRF.

4.4 FOG CRF Training

We employ Maximum Likelihood Estimation (MLE) and a numerical optimization technique to learn the model parameter w by maximizing the conditional log-log likelihood of the training data. To avoid over-fitting, we perform regularization through the optimization of a penalized likelihood using a Gaussian prior with a variance 0.5. We then perform gradient ascent to maximize the log likelihood. We compute the gradient using Forward-Backward algorithm and address the optimization task by employing the limited-memory BFGS [9]. To predict an FOG episode from its observation sequence O , our CRF utilizes the Viterbi algorithm to compute the likelihood probability that an observation sequence O would yield a given movement output label. The output movement label with the maximum likelihood probability is considered as the predicted movement class.

5. EXPERIMENTS

In this section, we present the results of the empirical evaluation of our FOG predictor. We conduct our experiments on an Intel PC with 8GB RAM. Our FOG prediction framework is implemented in Java. As previously alluded, we utilize the Parkinson’s disease accelerometer dataset described in Section 2.1 to perform our experiments. As a recap, the dataset has two output classes. Namely, the normal and the FOG class. Our objective is to predict from the low level accelerometer time series if a patient’s movement is normal or an FOG episode. During our experimental evaluations, to investigate the performance of our technique, we emphasize on the ability of our framework to detect FOG after τ seconds from its onset, where τ ranges from 2 to 6 seconds. In addition, we employ standard data mining evaluation metrics like precision, recall and F1-measure to evaluate the effectiveness of our technique.

5.1 Dataset Organization

The PD accelerometer dataset was extracted from 10 PD patients. [2] mentioned that Patient 4 and Patient 10 did

Patient 1 (H&Y Stage 3)	Codebook Size = 32			Codebook Size = 64		
	Precision	Recall	F1-Measure	Precision	Recall	F1-Measure
Normal	100	95.52	97.71	100	95.52	97.71
FOG	50	100	66.67	50	100	66.67
Overall	95.71			95.71		
Patient 8 (H&Y Stage 4)	Codebook Size = 32			Codebook Size = 64		
	Precision	Recall	F1-Measure	Precision	Recall	F1-Measure
Normal	86.36	90.48	88.37	85.71	85.71	85.71
FOG	66.67	57.14	61.54	57.14	57.14	57.14
Overall	82.14			78.57		
Patient 9 (H&Y Stage 2)	Codebook Size = 32			Codebook Size = 64		
	Precision	Recall	F1-Measure	Precision	Recall	F1-Measure
Normal	92.53	96.88	94.66	94.55	96.3	95.41
FOG	71.42	50.0	58.82	75.0	66.67	70.59
Overall	90.54			92.06		

Table 1: Window Size = 512 : FOG Evaluation for Patient 1, Patient 8, Patient 9.

not experience any FOG episode during the 8.5 hours period when the data was collected. As a result, we exclude the multi sensor accelerometer data from Patient 4 and Patient 10, and conduct our experiments using data from 8 PD patients. We train and test our FOG predictor for a given patient by using only the accelerometer data collected from the patient. Specifically, we place all the 3D accelerometer readings of a single user in a given file. We then partition the file into two sets. These include, the training set and the test set. We allocate 75% of the data to the training set while the remaining 25 % is used as the test set. We train our model on the training set while the test set is employed to predict a normal movement or FOG episode.

5.2 FOG Prediction

We perform our experiments using the approximation and detail wavelet sub-band energies (i.e., $a_4, d_4 \dots d_1$) as wavelet feature vectors. We observe that the performance of our predictor depends on several parametric settings such as the *Window Size* (w) and the *Codebook Size* L . We experimented with codebook sizes of $L = 32$ and $L = 64$. The *Window Size* (w) refers to the length of the multi sensor accelerometer time series that has to be segmented before wavelet transform. That is, to extract feature vectors using wavelet transform, we first segment raw accelerometer signals of a given class into a defined window size. Since we utilize MODWT, the window size must not be to the power of 2.

We select several window sizes depending on τ . Our aim is to predict FOG, τ seconds after its onset. The PD accelerometer dataset has a sampling rate of 64Hz. From the dataset, we observe that the timestamps after every four accelerometer readings is 47 milliseconds. This means 170 points correspond to accelerometer readings of $\tau = 2$ seconds. A window size of $w = 170$ is therefore used to measure our prediction performance within 2 seconds. We also perform experiments with $w = 256$ and $w = 512$ which correspond to our prediction performances within approximately 3 seconds and 6 seconds, respectively.

Towards this end, throughout this section, we investigate our prediction based on the window sizes of $w = 170, 256, 512$. For each window size, we analyze how the codebook sizes of $L = 32$ and $L = 64$ affects the prediction performance. In addition, [2] indicated that their technique had a lower performance on FOG detection for Patient 1 and Patient 8, because Patient 1 has a different walking style that made it difficult for their technique to recognize walking from very short FOG episode, whereas Patient 8 is a patient with the most advanced stage of Parkinson’s Disease and faces the greatest challenge during walking. As a result of this, we elaborately evaluate our FOG predictor on PD patients based on the H&Y ratings of their PD stages. Patient 9 has stage 2 PD, while Patient 1 and Patient 8 are at stage 3 and 4, respectively. The severity of the PD increases with an increase in the H&Y rating. Hence, we report our empirical evaluation for Patient 1 and Patient 8 to demonstrate the effectiveness of our predictive model on Parkinson’s disease patients with advanced movement disorder. Also, we present our result for Patient 9, who has an earlier stage Parkinson’s Disease.

Also, as previously mentioned, we report the precision ($Precision = TP/(TP + FP)$), recall ($Recall = TP/(TP + FN)$) and the F1-Measure of our prediction results; where TP, TN, FN and FP denote True Positive, True Negative, False Negative and False Positive, respectively. The F1-Measure is the harmonic mean of the precision and recall. It is given by

$$F1 - Measure = \frac{2Precision \times Recall}{(Precision + Recall)}$$

Besides, the overall performance of the prediction is given by

$$Overall = \frac{correct}{(correct + incorrect)}$$

where *correct* denotes the total number of correctly predicted labels and *incorrect* refers to the total number of incorrectly predicted labels. For our FOG prediction settings, because the vast majority of the PD accelerometer time se-

Patient 1 (H&Y Stage 3)	Codebook Size = 32			Codebook Size = 64		
	Precision	Recall	F1-Measure	Precision	Recall	F1-Measure
Normal	97.69	94.78	96.21	95.49	94.78	95.13
FOG	36.36	57.14	44.44	12.5	14.29	13.33
Overall	92.91			90.78		
Patient 8 (H&Y Stage 4)	Codebook Size = 32			Codebook Size = 64		
	Precision	Recall	F1-Measure	Precision	Recall	F1-Measure
Normal	83.33	95.24	88.89	87.5	83.33	85.37
FOG	77.78	46.67	58.33	58.82	66.67	62.5
Overall	82.46			78.95		
Patient 9 (H&Y Stage 2)	Codebook Size = 32			Codebook Size = 64		
	Precision	Recall	F1-Measure	Precision	Recall	F1-Measure
Normal	91.89	92.73	92.31	93.58	92.73	93.15
FOG	57.89	55.0	56.41	61.9	65.0	63.41
Overall	86.92			88.46		

Table 2: Window Size = 256 : FOG Evaluation for Patient 1, Patient 8, Patient 9.

ries comprises of normal movement time series, while FOG time series appears rarely, it is essential to verify the percentage of positive rarely occurring FOG episodes that are correctly detected by the predictor. This can be captured by investigating the recall of the FOG label. Hence, in the next section, we will emphasize and highlight the recall of the FOG label.

5.3 Prediction with Window Size of 512

Table 1 depicts our prediction results of Patient 1 for a window size of $w = 512$, when using different codebook sizes. For $L = 32$, we observe that our technique delivers an optimal recall of 100 % for the FOG label. The normal label attains a 95.52 % recall.

For the normal label, our approach achieve a precision of 100% and an F1-Measure of 97 .71 %. The FOG label has a 50 % precision and a 66.67 % F1-Measure. We should note that the drop in precision here is as a result of the submountable amount of normal movement accelerometer time series when compared to the few FOG time series, thereby leading to an increase in the False Positives. We increase the codebook size to $L = 64$ and the result does not change (i.e., exactly similar to that of $L = 32$) as can be seen in Table 1. A similar experiment with the same experimental settings was conducted on Patient 8, who has the most advanced stage of Parkinson’s disease. We notice a 90.48 % recall for the normal label and a lowered recall of 57.14 % for the FOG label. Maybe the lowered FOG recall may have resulted from the advanced stage of the patient’s PD. This FOG recall can be improved by exploring different combinations of wavelet feature vectors for stage 4 PD patients. However, the overall prediction performance for Patient 8 is 82.14 %. On the other hand, an elevated precision and F1-Measure of 86.36 % and 88.37 % are achieved for the normal label. In comparison to Patient 1, the FOG label has a 16 % increase of precision. The recall and F1-Measure of the FOG label of Patient 8 are 57.14 % and 61.54 %, respectively. Table 1 shows the results when the codebook size is increased to $L = 64$. Increasing the codebook size leads to a

3.57 % decrease in the overall prediction performance.

The detail prediction results of Patient 9 are illustrated in Table 1 also. For a codebook size of $L = 32$, our technique delivers a recall of 96.88 % and a precision of 92.53 % for the normal label. The FOG label yields a 50 % recall and a precision of 71.42 %. For this patient, increasing the codebook size to $L = 64$ results in the increase of the overall prediction performance from 90.54 % to 92.06 %.

5.4 Prediction with Window Size of 256

We use a window size of 256 samples during wavelet transform to test FOG predictions within 3 seconds from an FOG episode’s onset. Table 2 illustrates the prediction results. First, we notice that a decrease in window size from $w = 512$ to $w = 256$ leads to an erosion in prediction performance. Specifically, for $L = 32$, our predictive model produces an overall prediction performance of 92.91% for Patient 1. This is lower than that of $w = 512$ for the same patient. From the prediction confusion matrix, the normal label produces precision, recall and F1 measure of 97.69 %, 94.78% and 96.21 %, respectively. On the other hand, the FOG label outputs a recall of 57.14%. Its corresponding precision and F1-measure are 36.36% and 44.44 %, respectively. The table also illustrates the prediction results for the codebook size of $L = 64$. We observe an approximately 2% decrease of the overall prediction performance to 90.78 %.

For Patient 8, our technique achieves an overall performance of 82.46 % for $L = 32$, while for $L = 64$, it yields an overall prediction performance of 78.95 %. Also, for this settings, the FOG label shows a precision of 77.78 % for a codebook size of $L = 32$, but when we increased the codebook size to 64, we noticed a drop in precision to 58.823 %. This shows that a codebook size of $L = 32$ performs better. In contrast, for Patient 9, an increase in the codebook size from $L = 32$ to $L = 64$ improves the overall prediction performance from 86.92% to 88.46%. In particular, for $L = 32$, the normal and FOG labels deliver a precision of 91.89 % and 57.89 %, respectively. Also, the increase in codebook size prompts the precision to increase to 93.58 % and 61.9%,

Patient 1 (H&Y Stage 3)	Codebook Size = 32			Codebook Size = 64		
	Precision	Recall	F1-Measure	Precision	Recall	F1-Measure
Normal	97.89	92.08	94.9	97.42	93.56	95.45
FOG	30.43	63.64	41.18	31.58	54.55	40.0
Overall	90.61			91.55		
Patient 8 (H&Y Stage 4)	Codebook Size = 32			Codebook Size = 64		
	Precision	Recall	F1-Measure	Precision	Recall	F1-Measure
Normal	77.61	81.25	79.39	80.6	84.38	82.44
FOG	36.84	31.82	34.15	47.37	40.91	43.90
Overall	68.60			73.26		
Patient 9 (H&Y Stage 2)	Codebook Size = 32			Codebook Size = 64		
	Precision	Recall	F1-Measure	Precision	Recall	F1-Measure
Normal	88.13	85.45	86.77	88.69	90.30	89.49
FOG	31.43	36.67	33.85	40.74	36.67	38.6
Overall	77.95			82.05		

Table 3: Window Size = 170 : FOG Evaluation for Patient 1, Patient 8, Patient 9.

respectively.

5.5 Prediction with Window Size of 170

A short window size of 170 samples corresponds to the accelerometer time series for 2 seconds. Table 3 shows the empirical prediction results for Patient 1, Patient 8 and Patient 9 using a window size of 170 and codebook sizes of $L = 32$ and $L = 64$. Patient 1 attains an overall performance of 90.61%. The best overall prediction performances of our technique on Patient 8 and Patient 9 are 73.26% and 82.05% respectively. Despite the good overall prediction performances for such a short window size of $w = 170$, a detail look at the FOG label recalls for both $L = 32$ and $L = 64$ show a drop in the recalls. Specifically, a maximum FOG label recall of 63.64 % is obtained for Patient 1, while a minimum recall of 31.82 % is recorded for Patient 8. The latter is a sharp drop when compared to the 100% recall for $w = 512$. The main reason for this decrease in the FOG recall is caused by the decrease in window size. Using fewer samples decreases the frequency resolution at which we can examine the signal during wavelet transform. Besides, it also leads to the production of lesser salient regions in the wavelet modulus maxima, which is pivotal in providing unique signature features, that can be utilized to distinguish FOG signals from normal movement signals.

5.6 Discussions

Our major take aways from the experiments reported in Table 1 - Table 3 are as follows. For a short window size of $w = 170$, a large codebook size of $L = 64$ yields the best overall prediction result for PD patients at all stages. For longer window sizes (i.e., $w = 256$ and $w = 512$), we observe that the choice of the codebook size strongly depends on the patients PD stages. Specifically, a codebook size of $L = 64$ works better for PD patients at stage 1, whereas a codebook size of $L = 32$ performs better for advanced stage PD patients (i.e., stage 3 and 4) as shown in Table 1 and Table 2.

For all window sizes, we observe that our FOG predictor delivered the lowest results for the patient with the most severe stage of PD (i.e., Patient 8). In addition, we notice that as the window size increases, our predictive model performs better. Also, for a short window size of 170, our

F1-Measures range from 38% to 43%. Based on wavelet theory, if the accelerometer sensors sampling rate is increased such that at least 512 samples can be taken within 2 seconds, we believe our framework, which employs wavelet can produce near optimal FOG prediction results. Finally, we show that our framework formidably predicts FOG by yielding the best overall performances of 95.71%, 92.91% and 91.55% for $w = 512$, $w = 256$ and $w = 170$, respectively.

6. CONCLUSIONS

We propose a novel predictive model for FOG prediction that employs wavelets and CRF. We devise a new effective approach to select unique signature wavelet feature vectors, which are capable of distinguishing FOG time series from normal movement time series. We craft a CRF-based FOG predictive model that taps these signature feature vectors to learn the underlying characteristic of FOG and normal movement time series of Parkinson’s disease patients. Then, during prediction, our predictive model utilizes the learned patterns to predict FOG episodes with high veracity. We demonstrate through numerous experiments that our technique predicts FOG with an overall performance of over 90%, depending on the window size.

7. REFERENCES

- [1] Marc Bächlin, Jeffrey M. Hausdorff, Daniel Roggen, Nir Giladi, Meir Plotnik, and Gerhard Tröster. Online detection of freezing of gait in parkinson’s disease patients: A performance characterization. In *Proceedings of the Fourth International Conference on Body Area Networks, BodyNets ’09*, 2009.
- [2] Marc Bächlin, Meir Plotnik, Daniel Roggen, Inbal Maidan, Jeffrey M. Hausdorff, Nir Giladi, and Gerhard Tröster. Wearable assistant for parkinson’s disease patients with the freezing of gait symptom. *Trans. Info. Tech. Biomed.*, pages 436–446, 2010.
- [3] Bastiaan Bloem, Jeffrey Hausdorff, Jasper Visser, and Nir Giladi. Falls and freezing of gait in parkinson’s disease: A review of two interconnected, episodic phenomena. *Movement Disorders*, 2004.

- [4] Heiko Braak, Udo Rueb, Daniele Sandmann-Keil, Wei Ping Gai, R.A. de Vos, Jansen Steur, K Arai, and E Braak. Parkinson's disease: affection of brain stem nuclei controlling premotor and motor neurons of the somatomotor system. *Acta Neuropathologica - ACTA NEUROPATHO*, 2000.
- [5] Stanley Fahn. Description of parkinson's disease as a clinical syndrome. *New York Academy of Sciences.*, 2003.
- [6] A M Ardi Handojoseno, James M Shine, Tuan N Nguyen, Yvonne Tran, Simon J G Lewis, and Hung T Nguyen. The detection of freezing of gait in parkinson's disease patients using eeg signals based on wavelet decomposition. *Conf Proc IEEE Eng Med Biol Soc*, 2012.
- [7] John D. Lafferty, Andrew McCallum, and Fernando C. N. Pereira. Conditional random fields: Probabilistic models for segmenting and labeling sequence data. In *ICML '01*, 2001.
- [8] Y. Linde, A. Buzo, and R.M. Gray. An algorithm for vector quantizer design. *Communications, IEEE Transactions on*, 1980.
- [9] Dong C. Liu and Jorge Nocedal. On the limited memory bfgs method for large scale optimization. *Mathematical Programming*, 1989.
- [10] S. G. Mallat. A theory for multiresolution signal decomposition: The wavelet representation. *IEEE Trans. Pattern Anal. Mach. Intell.*, 1989.
- [11] Steven Moore, Hamish MacDougall, and William Ondo. Ambulatory monitoring of freezing of gait in parkinson's disease. *Journal of neuroscience methods*, 2008.